AN EVALUATION OF DIGILTAL ANTI-ALIASING FILTER FOR SPACE TELEMETRY SYSTEMS

Alison de Oliveira Moraes[(1)], José Antonio Azevedo Duarte [(1)], Sergio Fugivara[(1)]

[(1)]Comando-Geral de Tecnologia Aeroespacial,
Instituto de Aeronáutica e Espaço, Praça Mal. Eduardo Gomes, 50
Vila das Acácias, 12228-904 – São Jose dos Campos – São Paulo – Brazil
Email:aom@iae.cta.br; duarte@iae.cta.br; and fugivara@iae.cta.

ABSTRACT

The necessity of accelerometer sensors on launching vehicle and sounding rockets generally presents a concern for designing the telemetry system, due to the amount of bandwidth required to represent this kind of data. Commercially available sensors and conditioning amplifiers are not band-limited to frequencies of interest; and the usually analog anti-aliasing filtering techniques fails to perform an effective band limiting in PCM data acquisition system. These factors make even more difficult the managing of high dynamics sensor in traditional telemetry systems. This work reports an investigation about using digital anti-aliasing filter for data from accelerometer sensors in order to optimize the bandwidth of rocket telemetry systems.

1. INTRODUCTION

The use of accelerometer sensors on launching vehicle and sounding rockets is necessary to describe a complete dynamic performance of a flight. However, this kind of data generally requires a large bandwidth of the telemetry system. Besides, the commercially available sensors and conditioning amplifiers are not band-limited to frequencies of interest; and the usually analog anti-aliasing filtering techniques in a PCM data acquisition system fails to perform an effective band limiting. To reduce the effects of the aliasing due to the limitation described above, the PCM encoder usually oversamples the data from this kind of sensor. This process results in an increasing of the bit rate. In this work, an evaluation of the use of digital anti-aliasing filter is made and applied to accelerometer data before the PCM encoder has acquired it. Using a finite impulse response (FIR) filter, with a frequency response almost ideal, the sampling rate is reduced, with small increases in size, weight, and power of the onboard hardware. Results from tests with digital anti-aliasing filter, are analyzed and compared to traditional accelerometer data filtered by an analog filter following by an oversampling in the PCM encoder. Extending this analysis, these results are also compared to an accelerometer data acquired with ground system instrumentations where its sample rate and quantization resolution are much higher than any space telemetry system. The analyses showed that digital anti-aliasing filters present good results, making possible the replacement of the traditional measurement of accelerometer data for the proposed one. With this proposed filter in an onboard telemetry system is possible to enhance the performance of a typical sampling system so that it approaches Nyquist rate, and as consequence effectively reducing the amount of bits required in the telemetry system to represent this information. Therefore, the reduction in the amount of bits to represent this sort of information can be relevant in telemetry links with bandwidth limitations.

2. DATA SAMPLING

According to Nyquist–Shannon sampling theorem, an analog signal, $s(t)$, can be perfectly reconstructed based on samples of this analog signal. The condition for this perfect reconstruction is that the sample frequency, f_s, must be higher than twice the maximum frequency, B, of $s(t)$. So the analog signal must be bandlimted with $S(f)=0$ for $B>f_s/2$. The block diagram of a sampling system is show in Figure 1.

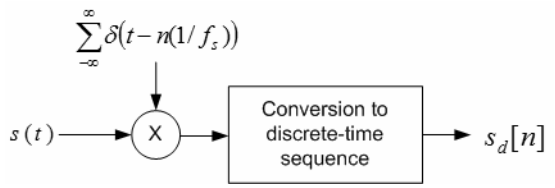

Figure 1. The process of continuous to discrete time conversion.

The Fourier transform of $s(t)$ and $s_d[n]$ are show respectively in Figure 2 (a) and (b). The difference between both spectrums is the fact that $S_d(f)$ is periodic in the frequency domain. Based on the dashed line in Figure 2 (b), it is possible to recover $s(t)$, applying an ideal lowpass filter on $s_d[n]$. This ideal lowpass filter is a pulse in the frequency domain with width of $2B$. In the time domain the impulse response of this ideal filter is given by:

$$h(t) = \sin\left(\pi t/(1/f_s)\right)/\pi t/(1/f_s) \qquad (1)$$

Proc. '19th ESA Symposium on European Rocket and Balloon Programmes and Related Research, Bad Reichenhall, Germany, 7–11 June 2009 (ESA SP-671, September 2009)

Then, the process of recovering the original signal *s(t)* based on the sequence of samples of $s_d[n]$ is given by:

$$s_r(t) = \sum_{-\infty}^{\infty} s_d[n] \frac{\sin\left(\pi(t - n(1/f_s))/(1/f_s)\right)}{\left(\pi(t - n(1/f_s))/(1/f_s)\right)} \quad (2)$$

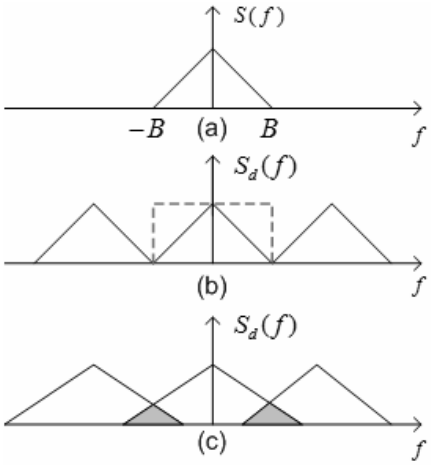

Figure 2. Fourier transform showing the effects of sampling .

The process of reconstruction of *s(t)* using $s_d[n]$ using Eq. (2) is called interpolation. The ideal interpolation process is show in Figure 3.

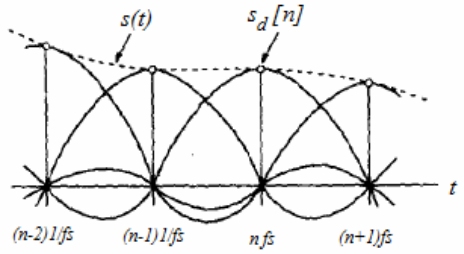

Figure 3. Signal reconstruction based on ideal interpolation [2].

Unfortunately, devices designed for analog to digital conversion are limited and it is not possible to implement the ideal lowpass filter for reconstruction process. These factors avoid the perfect reconstruction of *s(t)* based on the samples of $s_d[n]$. Despite these factors it is possible to achieve good approximations for *s(t)*.

As it has been shown, all the theory that allows decomposing the continuous signal and reconstruct that based on its samples, considers that the signal *s(t)* is bandlimited. However, in the real world, there are no bandlimited signals. When the signal is not bandlimited, the periodic copies on the spectrums of $S_d(f)$ overlap each other and the signal is not recoverable any more. This process is called aliasing and it is shown in Figure 2 (c). In practice, this effect is always present, and it has to be managed to guaranty the minimum distortion.

The task of minimizing the effects of aliasing on electronic systems is done by anti-aliasing filter.

3. ANTI-ALIASING FILTER

In most measurement systems, the anti-aliasing filter is implemented with a passive analog filter. More sophisticated systems work with active analog filters that are more effective if compared to the passive ones. To be effective, an analog active filter needs to have a high order that results in a large number of components and higher price. Besides, even a high order analog filter would fail to eliminate elements close to the maximum frequency *B*. This happens because the analog filter does not present a sharp response close from the cut-off frequency.

In this work, a digital FIR (Finite Impulse Response) filter is used to perform the task of anti-aliasing filter. The FIR filters are chosen by the fact that they are always stable because all their poles are in the origin. Besides this kind of filter presents a linear phase response which is important to analyze data in the time domain.

The use of a digital FIR filter allow to set the cut frequency close to the value *B*, with a minimum ripple and no attenuation close to this bound like in analog filter. But the main advantage of this kind of filter is the sharpness of the transition between the cut frequency and the rejected band. Figure 4 shows an example of the frequency response of this filter.

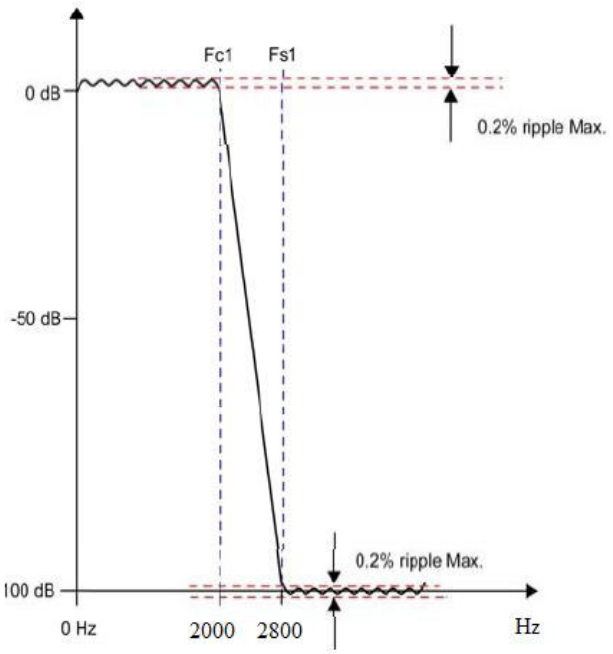

Figure 4.Frequency response of the digital anti-aliasing filter of this work.

The strategy in this work is to take the advantage of the frequency response of the digital filter to consider the measured signal as bandlimited. The value of *B* must be adequate to the region of the beginning of the rejection band. With this approach, the telemetry system can acquire the data with a small sample frequency. Besides the data resulted from this process is expected to be the best approximation for the original measured signal.
The basic architecture of the digital anti-aliasing filter used in this work is presented in Figure 5.

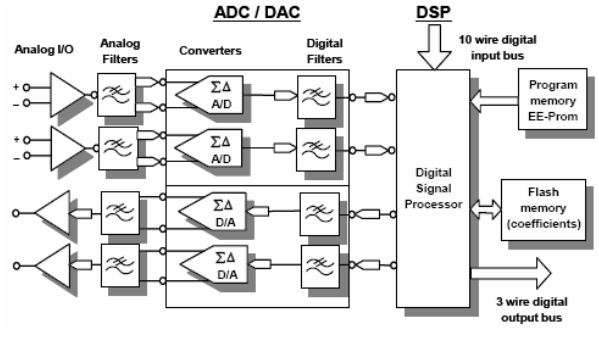

Figure 5. Architecture of the digital anti-aliasing filter.

4. METHODOLOGY OF THE MEASUREMENTS

The accelerometer used in this test was placed on the motor adapter of the VSB-30 sounding rocket during the dynamic acceptance testing of this module. Figure 6 illustrates the motor adapter and shows the position where the accelerometer has been fixed.

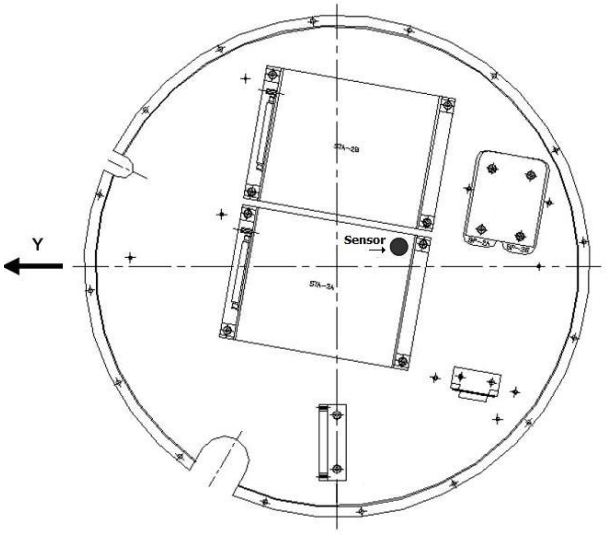

Figure 6. Motor Adapter.

In order to analyze the effectiveness of the digital anti-aliasing filter for accelerometer data, it has been considered the diagram of Figure 7 for the tests.

The signal from one monoaxial accelerometer, *A(t)*, is first amplified and filtered by a traditional 6 poles analog anti-aliasing filter. This amplified and filtered version of the accelerometer signal, *X(t)*, is than acquired by the PCM encoder with a sample frequency 10, 5 and 2.5 times the maximum frequency of *A(t)*. In parallel, the signal *X(t)*, is applied to the FIR filter, generating the signal *W(t)*. The signal *W(t)* is also applied to the PCM encoder to be acquired with a sample frequency of 2.5 times.

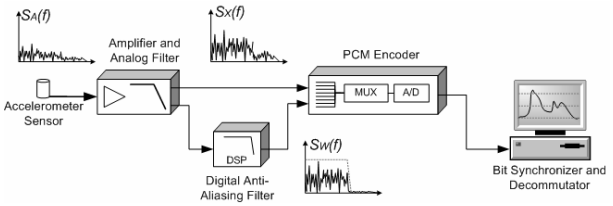

Figure 7. Block diagram of the measuring system.

The reasons for these sample frequencies can be justified in the following way. In a traditional rocket telemetry system, the accelerometer data is sampled between 4 and 5 times the maximum frequency, which the sensors can respond. This is why one channel was set to the sample frequency of 5 times, which is considered the standard ratio for this kind of data. Another PCM channel has been acquired with a sample frequency of 10 times. This channel has been considered as an "onboard" reference for the telemetry measurements. Two PCM channel were set for the sample rate of 2.5 maximum frequency. These particular channels is the focus of this work, once that the intention is to compare the quality of the data with and without the digital anti-aliasing filter in a sample rate that is close to Nyquist bound.
Signals acquired by the PCM encoder were digitalized with 10 bits of quantization. The serial output data from the PCM encoder was processed by a telemetry ground station, which consists of PC based bit synchronizer and PCM decommutator. The result of this processing are four files, with the stochastic process $X_1[n]$, $X_2[n]$, $X_3[n]$ and $W[n]$. The files, with $X_1[n]$, $X_2[n]$, $X_3[n]$ contains the data related to X(t), sampled in 10, 5 and 2.5 times the maximum frequency of A(t). The process W[n] represents the discrete version of X(t) filtered by the digital filter. Figure 8 shows an example of *W[n]*.

5. RESULTS

In this section we present the results related to the accelerometer data during the dynamic acceptance tests. Figure 8 shows an example of the acquired data during the tests in the time domain.

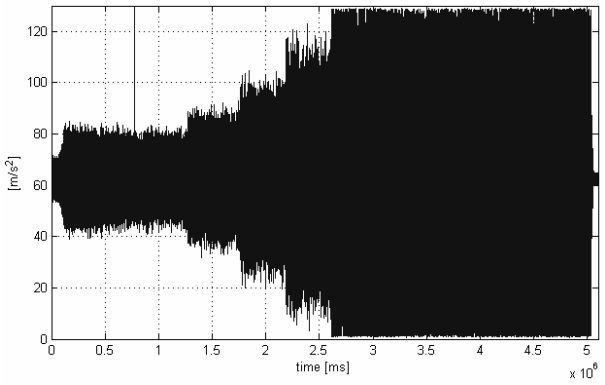

Figure 8. Signal $x_2[n]$.

During acceptance tests, an instrumentation ground system is the source of data, used to analyze the dynamical performance of the module. The data from this instrumentation ground system is also presented in this section as an auxiliary reference. This data is considered a "ground" reference because it has been acquired with a 32 bits of quantization and analog filter with 24 poles and a sample frequency that is 50 times higher than the maximum frequency of *A(t)*. Besides that, this instrumentation system is completely isolated from the onboard telemetry system. Thus, the signal might be considered the closest approximation of *A(t)*.
The results presented in this section are divided in two cases. The first case presents results related to a test where there is no interferences or noise outside from the bandwidth of interest. The second case presents an example where some kind of interference is present. This interference was not initially predicted in this research. It was from an unknown source and it was discovered during the analyses of the data for this work.
Before presenting the results, it is presented some assumption for the analyzes. The random vibration that the VSB-30 motor adapter module is submitted is generated by a shaker. The signal obtained from this test is considered a wide sense stationary. In this case, the power spectrum density, $S_W(f)$, of the stochastic process $W[n]$, is the Fourier transform of the autocorrelation function, $R_W[n_1-n_2]$, of the data sensor, defined by:

$$S_W(f) = \lim_{m\to\infty} \frac{1}{2m+1} \mathrm{E}\left[\left|W_m(f)\right|^2\right] \qquad (3)$$

where $\mathrm{E}\left[\left|W_m(f)\right|^2\right]$ is given by:

$$\mathrm{E}\left[\left|W_m(f)\right|^2\right] = \sum_{n_2=-m}^{m} \sum_{n_1=-m}^{m} R_W[n_1-n_2] e^{-j2\pi f(n_1-n_2)} \qquad (4)$$

and the autocorrelation function is defined by:

$$R_W[n_1-n_2] = \mathrm{E}\left[W[n_1]W^*[n_2]\right] \qquad (5)$$

The power spectrum density of the ground based instrumentation system is presented in Figure 9, as an example.

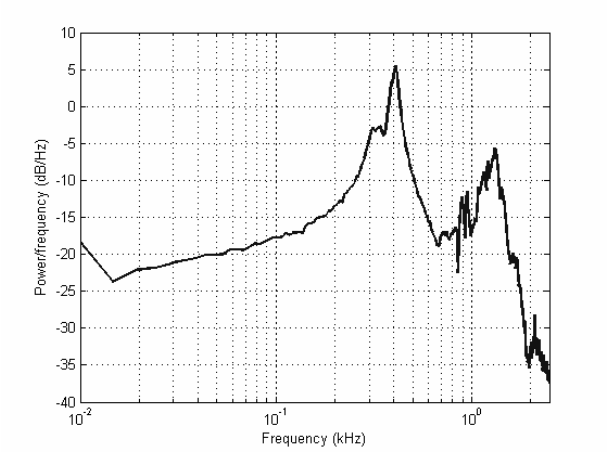

Figure 9. Power spectrum density of ground based instrumentation system for the second case.

First Case

The power spectrum density of $X_1[n]$, $X_2[n]$, $X_3[n]$ and $W[n]$ for the case where there is no interferences in the measurement system, during the test, are show respectively in Figures 10, 11 , 12 and 13.

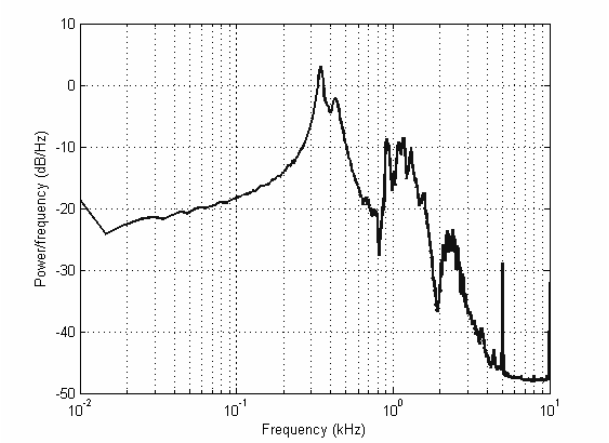

Figure 10. Power spectrum density of $X_1[n]$.

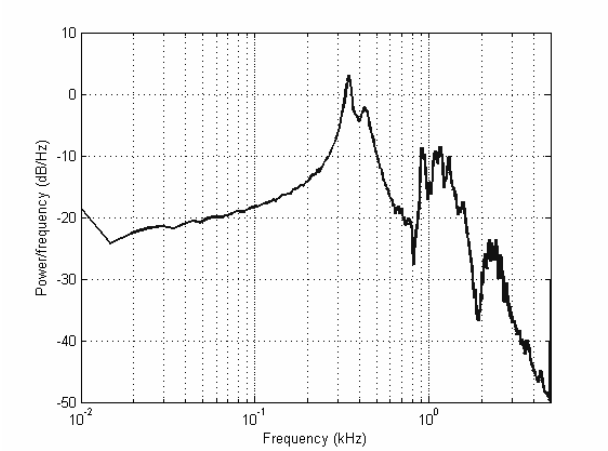

Figure 11. Power spectrum density of $X_2[n]$.

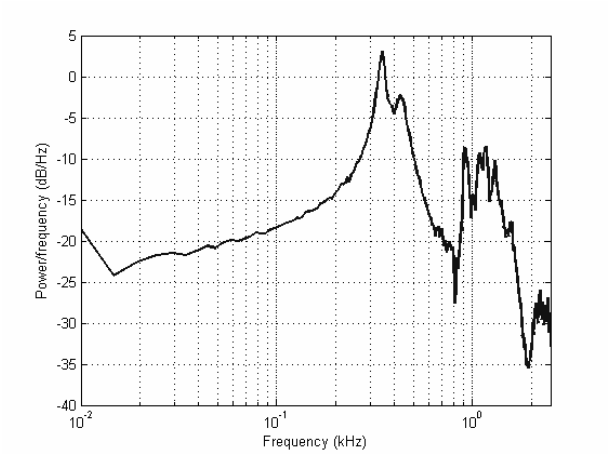

Figure 12. Power spectrum density of $X_3[n]$.

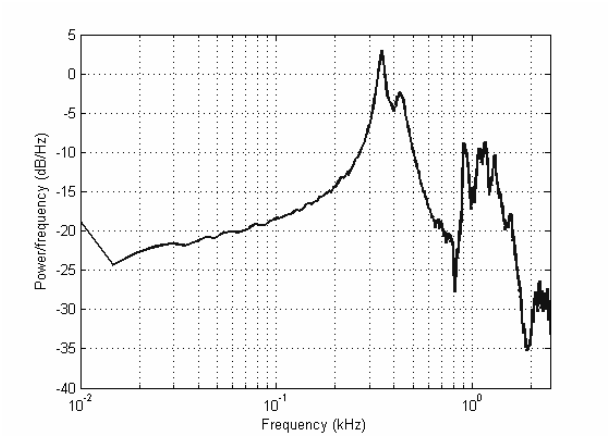

Figure 13. Power spectrum density of W[n].

Analyzing these results, it is possible to conclude that all the power spectrum densities are alike. The results from this case would suggest that if all the results are very similar, the best implementation for onboard telemetry system would be using only the accelerometer with its own amplifier and filter and a sample frequency close from 2.5*B*.

Second Case

The power spectrum density of $X_1[n]$, $X_2[n]$, $X_3[n]$ and $W[n]$ for the case with interference are show respectively in the Figures 14, 15, 16 and 17.

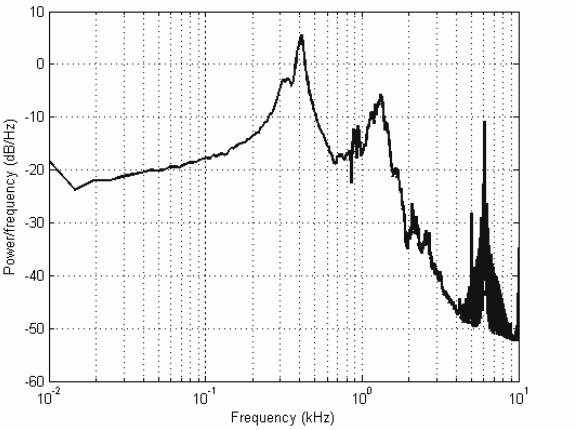

Figure 14. Power spectrum density of $X_1[n]$.

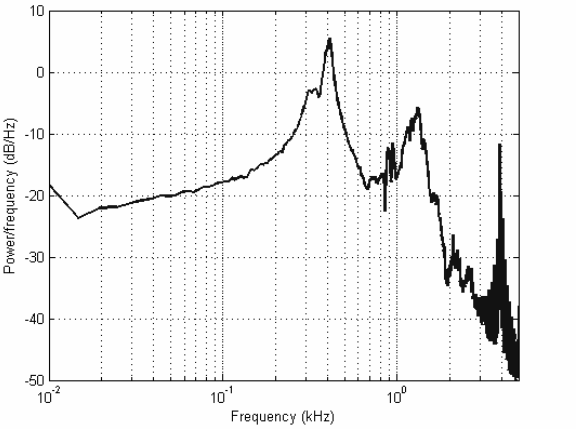

Figure 15. Power spectrum density of $X_2[n]$.

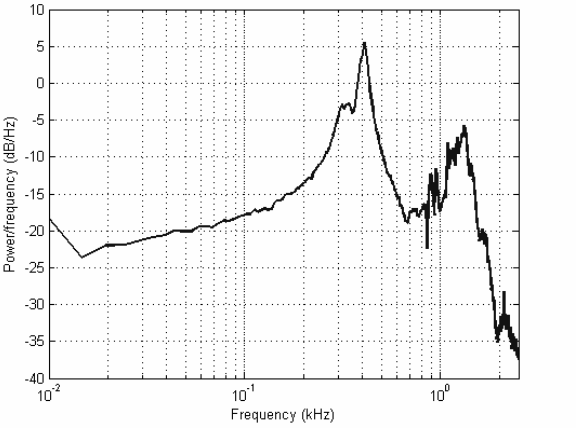

Figure 16. Power spectrum density of $X_3[n]$.

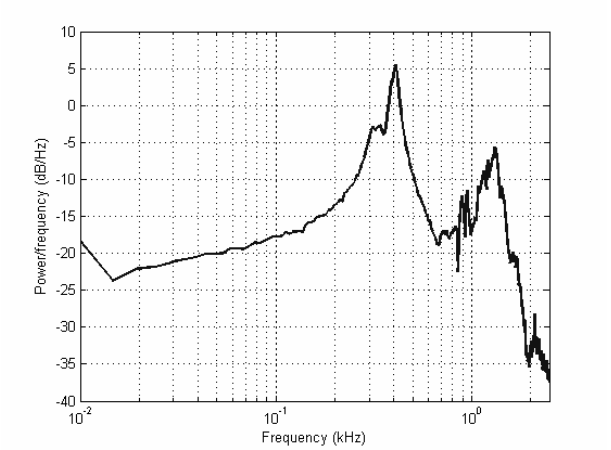

Figure 17. Power spectrum density of W[n].

In this case, it is possible to see an interfering signal together with the tested signal. In Figure 14, it is possible to see this signal present around 6kHz. Probably, this interfering signal is due to some kind of switching, maybe provided by other circuits present in the module or around, in the laboratory. Based on Figures 14, 15 and 16 it is possible to conclude that interferences can damage the quality of the data. In a flight, interference like that might difficult the analyses of the flight introducing to a wrong conclusion based on this kind of corrupted data.

6. CONCLUSION

Based on the first case, the solution of using only the accelerometer with its own amplifier and filter with a sampling rate close to Nyquist bound, seems to be perfect by the fact that there is no extra circuit onboard and the telemetry system is saving bits if compared with the traditional systems. However, when there is some kind of interference, as in the second case, this system will fail. Based on the second case, it was shown that some kind of interference, depending on the situation, might result in a wrong interpretation of the dynamical performance of the flight. The results from the second case allow the conclusion that the digital anti-aliasing filter presents good solution to guaranty the integrity of the data provided by the telemetry system during the flight. This result is more relevant if taking into account the aspect of save bits for the telemetry system.
As a future work, this filter will be tested in a sounding rocket to evaluate its performance in a real flight.

7. REFERENCES

1. Oppenheim AV, Shafer RW. *Discrete time signal processing*. Prentice Hall; Englewood Cliffs, NJ: 1982.
2. Proakis, J. G. *Digital communications*, 3. ed. New York: McGraw-Hill Inc., 1995.
3. Krishnan, V. *Probability and Random Processes*, 1. ed. New Jersey: John Wiley & Sons, 2006.